

Study, extension, and application of Floquet theory for quantum molecular systems in an oscillating field

Kent F. Milfeld and Robert E. Wyatt

Institute for Theoretical Chemistry and Department of Chemistry, University of Texas, Austin, Texas 78712

(Received 1 March 1982)

Floquet theory is applied to systems whose Hamiltonians are periodic in time. Specifically, the application deals with the sinusoidal Hamiltonians for the semiclassical approximation of the radiation—quantum-molecule interaction in an intense field. For these types of Hamiltonians new time symmetries are shown to exist in the Floquet solutions and consequently to yield three useful properties. Three formal approaches to the Floquet solutions are compared. Also the Floquet-state “mean energy” is shown to play the major role in the static part of the molecular-state energy fluctuations. Numerical application to the dynamics of the diatomic HF vibrotor shows multistate participation in both the one- and two-photon excitations, and “resonance interaction” between the one- and two-photon absorption is observed. Also, Magnus approximations to the exact numerical calculations show excellent agreement.

I. INTRODUCTION

Along with the advent of lasers, interest grew rapidly in semiclassical radiation theory as a viable approximation to the full quantum description of molecules in intense laser fields. Within the semiclassical approach, the molecular dynamics produced by the radiation-molecule interaction is investigated here for fields which are described classically and for molecules which are described quantum mechanically. The time-dependent Schrödinger equation can be integrated directly or approximated by analytic Magnus expressions to obtain the evolution of the system in the form of the fundamental propagator. Here, the expression “fundamental” denotes that the propagator is determined in the molecular-state representation and evolves from the initial field-free molecular states.

Floquet theory provides a unique functional form for a (Floquet) propagator which permits “exact” or approximate solutions for the semiclassical equations of motion without resorting to perturbation theory, the rotating wave approximation, or to a brute force integration for times greater than one oscillation of the field. Using the periodic form of the Floquet propagator, the problem can be reformulated with solutions and eigenvalues (in the form of Floquet characteristic exponents) which characterize and simply determine the dynamics. The periodicity also allows analytic expressions for time averages.

As far back as the 1880's, Floquet periodic solu-

tions of the semiclassical-type equations, first-order homogeneous differential equations having periodic (in time) coefficients, were studied by Floquet¹ and Poincaré.² Not until after the mid 1960's did the application of Floquet theory to quantum systems grow. The usefulness of the theory is evident by the diversity of its applications. Salzman,³ Chu and Reinhardt,⁴ and Chu⁵ have applied Floquet theory to hydrogen atom multiphoton ionization, while Leasure and Wyatt,⁶ and Leasure, Wyatt, and Milfeld⁷ have applied it to a “larger” system, the rotating diatomic. Floquet theory has even been used in the studies of molecular multiphoton dissociation by Leforestier and Wyatt (in one study, Floquet states were used in conjunction with *R*-matrix theory,⁸ and in the other, with the investigation of the optical potential⁹). Some of the earlier applications are given in a review of the quantum “two-level problem” by Dion and Hirschfelder,¹⁰ which also includes a description of the nine Floquet theorems.

More theoretically oriented studies including Floquet analysis (also known as the quasienergy method) have expanded the work of Shirley,¹¹ Ritus,¹² and Zeldovich¹³ to include slowly modulated oscillatory Hamiltonians,¹⁴ development of an extended Hilbert-space formalism,¹⁵ approximation of the propagator to simplify the dynamics,³ and investigation of a new notion of energy (“mean energy”),¹⁶ to name some examples.

In this study, both the theory and application of the Floquet formalism are extended. We begin in

Sec. II with a short review of the general properties of time-dependent Hamiltonians, propagators, and the application of Floquet theory to molecular dynamics. Also, the relationship between the Floquet and fundamental propagators is defined. In Sec. III new symmetries in the Floquet solutions for the semiclassical Hamiltonian are derived. These properties can be used to shorten computations. In Sec. IV, different Floquet formalisms are related, with an emphasis on the role of the Floquet characteristic exponents (or quasienergies). A new method is presented for correlating molecular energies to the Floquet characteristic exponents in multistate systems. Also, we introduce a measure of the molecular-state energy and find that the constant energy term is a linear combination of the Floquet state mean energies, while fluctuations are determined by the Floquet characteristic exponents. Presented in Sec. V are formal expressions for the Magnus propagator, up to fifth order, and a note on their derivation. Also, we have derived the third-order interaction picture, and the third- and fourth-order Schrödinger picture matrix elements using the Magnus approximation for the semiclassical Hamiltonian. Section VI contains numerical results for the HF vibrotor. Time-averaged one- and two-photon absorption probabilities are determined at various (IR) frequencies and intensities, along with time-dependent survival plots which show probability (and energy) exchange. Also included is a critical comparison of the Floquet characteristic exponents, propagators and mean energies as determined by both numerical integration and the Magnus approximation. Finally, multiphoton resonances are shown to directly affect the single-photon absorption in a physically measurable way. We end with conclusions in Sec. VII.

II. PROPAGATORS FOR PERIODIC HAMILTONIANS

The sinusoidal (periodic) time dependence introduced by the classical radiation field sets apart a genre of Hamiltonians with propagators amenable to Floquet analysis. The introduction of Floquet theory into the dynamics recovers the Hamiltonian periodicity, which is lost in the fundamental propagator, through the generation of the Floquet propagator; the Floquet propagator is then used to efficiently determine the fundamental propagator for all times.

The sinusoidal time-dependent Hamiltonian (ω is the field frequency)

$$H(t) = H_0 + V \cos(\omega t), \quad (1)$$

where H_0 and V are time-independent operators (or matrices), is used to describe quantum systems (such as those which occur in NMR and IR experiments) interacting in the dipole approximation with a classically oscillating monochromatic linearly polarized field. In the molecular-state representation H_0 is the diagonal matrix E of molecular energies and V represents the scalar product of the electric field magnitude-polarization vector ($\vec{\epsilon}$) and the molecular dipole moment ($\vec{\mu}$). Since we are particularly interested in IR laser-induced molecular excitation, within a single electronic manifold, the formalism will be directed and couched in terms of multistate vibrational excitations (of vibrotors). Throughout, a *capital symbol* will denote an operator or a *matrix* (with the corresponding small doubly subscripted symbols as matrix elements, and singly subscripted symbols as vectors) in the molecular-state representation, unless stated otherwise or the notation's meaning is obvious.

The time propagator is a linear operator $U(t | t_0)$ which transforms an initial state $|\Psi(t_0)\rangle$ at time t_0 into state $|\Psi(t)\rangle$ at time t : $|\Psi(t)\rangle = U(t | t_0)\Psi(t_0)\rangle$. The propagator has special properties which can be attributed to its unitarity and to its initial conditions.

The unitary condition and the time multiplication relations are

$$U^\dagger(t | t') = U^{-1}(t | t') = U(t' | t) \quad (2)$$

and

$$U(t | t'') = U(t | t')U(t' | t''), \quad (3)$$

respectively.¹⁷ The evolution of $U(t | t_0)$ is determined by the time-dependent Schrödinger equation:

$$i\hbar \frac{\partial}{\partial t} U(t | t_0) = H(t)U(t | t_0), \quad (4)$$

where the integral equation equivalent to Eq. (4) is

$$U(t | t_0) = 1 - (i/\hbar) \int_{t_0}^t H(t')U(t' | t_0)dt'. \quad (5)$$

The initial condition adopted for its physical significance and simplicity is

$$U(t_0 | t_0) = 1, \quad t_0 = 0 \quad (6)$$

which forces the propagator $U(t | t_0)$ to determine the evolution of the linearly independent molecular-state eigenvectors; $U(t | t_0)$ is the *fundamental propagator*.

The propagator solution of Eq. (4) [or Eq. (5)], can be obtained by numerical integration using the

initial (fundamental) condition of Eq. (6). But it is advantageous to transform or analyze the Hamiltonian for possible constants which have physical significance and determine the dynamics in a simple way. For example, in a conservative (molecular) system the constants are the energies and the system evolves according to them. When $V=0$ in Eq. (1), the propagator in the molecular-state representation is simple,

$$U(t | t_0) = \exp[-i\kappa(t - t_0)/\hbar], \quad \kappa \neq \kappa(t) \quad (7)$$

where $\kappa = E$ is the diagonal matrix of molecular energies.

It is the periodic form of $H(t)$ which permits the use of the Floquet propagator^{1,18} having the Floquet characteristic exponents (FCE) as constants. Unlike the energy constants in Eq. (7), which solely evolve the stationary states of a time-independent Hamiltonian, the Floquet characteristic exponents neither evolve the system by the same exponential form nor are they a result of a transformation to stationary states. The FCE are a consequence of the time dependence of the Floquet states and the periodic boundary conditions. For a molecular system of N states, there are N -independent Floquet

states, each the product of a τ periodic factor [$\tau = 2\pi/\omega$ is the optical cycle (oc)] and an exponential of a pure imaginary term. The Floquet propagator elements are of the form

$$f_{in}(t) = \phi_{in}(t \bmod \tau) e^{-i\mu_n \omega t}, \quad (8)$$

or in matrix notation

$$F(t) \equiv U^F(t | 0) = \Phi(t \bmod \tau) e^{-iM\omega t}, \quad (9)$$

where the superscript of $U^F(t | 0)$ indicates that it is the Floquet propagator. To be consistent with the standard convention ($\mu_n \omega$) is defined as the Floquet characteristic exponent [(FCE) Refs. 10, 11, and 19] and the arbitrary sign of the exponential argument is negative. We define the product $\mu_n \hbar \omega$ as the Floquet energy (FE), which is also called the quasienergy.¹⁴⁻¹⁶

Using Floquet theory, Shirley^{11,20} derived an expression for the fundamental propagator of Eq. (1). His approach employs a time-independent infinite matrix operator H_F called the Floquet Hamiltonian. Shirley's propagator elements connecting molecular states (i) and (n) are determined from a sum over a projection onto Fourier modes (m) with a corresponding phase factor [compare with Eq. (7)]:

$$U_{in}(t | t_0) = \sum_{m=-\infty}^{\infty} \langle im | \exp[-iH_F(t - t_0)/\hbar] | n0 \rangle e^{im\omega t}, \quad (10)$$

where the direct product $|im\rangle = |i\rangle |m\rangle$; $|i\rangle$ is a molecular state, and $|m\rangle$ is a Fourier expansion "state" [$\exp(im\omega t)$ is the basis function for $|m\rangle$]. The time independence of H_F was determined through the Fourier expansion of both the Floquet propagator and $H(t)$, in the molecular-state representation. These expansions, when substituted into the Schrödinger equation, result in an infinite recursion equation free of the time-dependent Fourier ($e^{im\omega t}$) terms. The infinite recursion is recast into the matrix eigenvector equation (45) with a double index over the molecular basis (i, n) and the Fourier coefficient basis (m, l). Computationally, the major task is then to diagonalize the infinite (actually truncated) matrix, which can be shown to give N -independent eigenvector solutions $|\lambda_{j0}\rangle$, and N Floquet eigenvalues λ_{j0} (for an N -molecular-state system; j ranges from 1 to N). In terms of the eigenvectors and eigenvalues, $U_{in}(t | t_0)$ is given by

$$U_{in}(t | t_0) = \sum_{mjl} \langle im | \lambda_{jl} \rangle e^{-i\lambda_{jl}(t - t_0)/\hbar} \langle \lambda_{jl} | n0 \rangle e^{im\omega t} \quad (11)$$

with eigenproperties,

$$\begin{aligned} \langle i, m+p | \lambda_{j, l+p} \rangle &= \langle i, m | \lambda_{j, l} \rangle, \\ \lambda_{jl} &= \lambda_{j0} + l\hbar\omega; \end{aligned} \quad (12)$$

p and l are integers. In the notation of Eqs. (8) and (9), which will be used throughout, the projection coefficients in Eq. (11) are

$$\langle im | \lambda_{n0} \rangle = \phi_{in}^m, \quad (13)$$

where $\{\phi_{in}^m\}$ are the Fourier expansion coefficients of $\phi_{in}(t)$;

$$\phi_{in}(t) = \sum_{m=-\infty}^{\infty} \phi_{in}^m e^{im\omega t}, \quad (14)$$

and

$$\lambda_{n0} = (\mu_n \omega) \hbar. \quad (15)$$

The most notable utility and attraction of the H_F formalism is its time independence and the similarity between its propagator expression, Eqs. (10) and (11), and that of the time-independent Hamiltonian of Eq. (7).

In their development of Floquet theory, Leasure

and Wyatt¹⁹ determined the Floquet characteristic exponents by evaluating $U(t | 0)$ at $t = \tau$ in Eq. (27) and incorporating the periodic condition of Eq. (9) to obtain the smaller $N \times N$ eigenvalue equation

$$\Phi^\dagger(0)U(\tau | 0)\Phi(0) = e^{-i2\pi M}. \quad (16)$$

[Compare Eq. (16) with Shirley's eigenequation (45) which has additional Fourier states.] Since the fundamental propagator is linearly related by $\Phi^\dagger(0)$ to the Floquet propagator in the equation

$$\begin{aligned} U(t | 0) &= U^F(t | 0)\Phi^\dagger(0) \\ &= \Phi(t \bmod \tau)e^{-iM\omega t}\Phi^\dagger(0), \end{aligned} \quad (17)$$

$U(t | 0)$ is determined for the first optical cycle and is then used in the inverted form of Eq. (17) to obtain $\Phi(t \bmod \tau)$. Also, note that for the Floquet

propagator, $U^F(t | 0)$, at $t=0$ the initial condition is fixed by Eqs. (9) and (16):

$$U^F(t=0 | 0) = \Phi(0). \quad (18)$$

In the $U\tau$ approach [named for the matrix in Eq. (16)], the Floquet energies are clearly seen as "dynamic boundary constraints" because they are determined by the fundamental propagator only at time τ .

To obtain $U(t | 0)$ for the first optical cycle, an integration of the coupled equations (4) to time τ provides an "exact" propagator, with numerical results limited only by the accuracy of the integrator and the availability of computation time. Also, the Magnus approximation²¹ can be used to provide an analytic unitary propagator of any desired order (Sec. V).

III. SYMMETRY AND OTHER PROPERTIES OF $\Phi(t)$

For the sinusoidal Hamiltonian, such as the semiclassical $H(t)$, or any Hamiltonian having the time dependence shown below in Eq. (19), the Floquet $\Phi(t)$ matrices have symmetry in time and, therefore, possess special properties. These properties, to be derived in this section, constitute a new extension to the Floquet theory for the periodic time dependence mentioned above. The derivations in this section may be used in a general fashion to analyze the effects that other periodic Hamiltonians have on the Floquet solutions and on the dynamics of the system.

Within the range $0 < t < \tau$, the symmetry in $H(t)$ about $t = \tau/2$,

$$H(\tau/2 - t) = H(\tau/2 + t), \quad (19)$$

is reflected in the fundamental propagator by the equation

$$U(\tau/2 - t | \tau/2) = U^*(\tau/2 + t | \tau/2). \quad (20)$$

One may arrive at this result by substituting $\tau/2$ and $t + \tau/2$ for t_0 and t , respectively, in the integral equation (5), and transforming the integral variable from t' to $t'' + \tau/2$ to obtain

$$U(\tau/2 + t | \tau/2) = 1 - i/\hbar \int_0^t H(\tau/2 + t'')U(\tau/2 + t'' | \tau/2)dt''. \quad (21)$$

By transforming t'' to $-t'$, changing the limit t to $-t$, replacing H by its equivalent in Eq. (19), and finally taking the complex conjugate of both sides of the equation, Eq. (21) becomes

$$U^*(\tau/2 - t | \tau/2) = 1 - i/\hbar \int_0^t H(\tau/2 + t')U^*(\tau/2 - t' | \tau/2)dt'. \quad (22)$$

Since $U(\tau/2 + t | \tau/2)$ and $U^*(\tau/2 - t | \tau/2)$ obey the same evolution equation [Eqs. (21) and (22)] and boundary conditions, they are equivalent expressions and Eq. (20) is proven.²²

Although $U(\tau/2 + t | \tau/2)$ has symmetry about $t = \tau/2$ [Eq. (20)], it is the fundamental propagator $U(t | t_0=0)$ which is required for the initial-to-final-state analysis. One would certainly want to know whether it, too, is symmetric about $\tau/2$ in the same sense as $U(\tau/2 + t | \tau/2)$, i.e., does $U(\tau/2 - t | 0) = U^*(\tau/2 + t | 0)$? Besides introducing symmetry into the dynamics, such a relation

would reduce by half the computational task of propagating over one optical cycle. Therefore, it is advantageous to see whether manipulation of $U(\tau/2 + t | \tau/2)$ leads to an expression of symmetry for $U(\tau/2 + t | 0)$.

By the time-ordered (multiplication) relation of Eq. (3)

$$U(\tau/2 + t | \tau/2)U(\tau/2 | 0) = U(\tau/2 + t | 0), \quad (23)$$

where, implicit in the equality, $U(\tau/2 | 0)$ is deter-

mined from the fundamental propagator $U(t|0)$ and the initial condition on $U(\tau/2+t|\tau/2)$ is $U^\dagger(\tau/2|0)$. Using Eq. (20) and the unitarity relation $U^\dagger(t|t')=U^{-1}(t|t')=U(t'|t)$ on the left-hand side (LHS) of Eq. (23) gives

$$U^*(\tau/2-t|\tau/2)U^\dagger(0|\tau/2)=U(\tau/2+t|0), \quad (24)$$

and by using the time multiplication relation again

$$U^*(\tau/2-t|0)C=U(\tau/2+t|0), \quad (25)$$

where

$$\begin{aligned} C &= U^*(0|\tau/2)U^\dagger(0|\tau/2) \\ &= U^T(\tau/2|0)U(\tau/2|0). \end{aligned}$$

Since, in general, $C \neq 1$, Eq. (25) precludes a simple symmetry relation in $U(\tau/2+t|0)$. However, the $t_0=0$ propagator for $\tau/2 \leq t \leq \tau$ [the right-hand side (RHS) of Eq. (25)] can be simply determined from the first half of the optical cycle through a product with the *constant matrix* C ; and, therefore, this procedure will reduce the computation time to nearly half. Also, the propagator at the end of the cycle may be self-consistently checked by the relation

$$C=U^T(\tau/2|0)U(\tau/2|0)=U(\tau|0), \quad (26)$$

which is determined by setting t to $\tau/2$ in Eq. (25).

The symmetry of the Floquet periodic matrix $\Phi(t)$ will now be determined from the propagator $U(t|t_0)$ through the defining equation

$$\Phi(t)e^{iAt}=U(t|t_0)\Phi(t_0)e^{iAt_0}, \quad (27)$$

where $a_{in} = -\delta_{in}\mu_n\omega$. We will derive three properties of the periodic solutions, $\Phi(t)$. First, by substituting $\tau/2-t$ and $\tau/2$ in Eq. (27) for t and t_0 , respectively, replacing the fundamental propagator by its equivalent in Eq. (20),

$$\Phi(\tau/2-t)e^{-iAt}=U^*(\tau/2+t|\tau/2)\Phi(\tau/2), \quad (28)$$

taking the complex conjugate of this equation and replacing t by $-\tau/2$ yields

$$\Phi^*(\tau)e^{-iA\tau/2}=U(0|\tau/2)\Phi^*(\tau/2), \quad (29)$$

which, by using the periodicity of Φ [i.e., $\Phi(\tau)=\Phi(0)$] and the propagator inverse, $U^{-1}(t|t')=U(t'|t)$, results in an equation with a familiar form:

$$U(\tau/2|0)\Phi^*(0)=\Phi^*(\tau/2)e^{iA\tau/2}. \quad (30)$$

Now, by Eq. (27),

$$U(\tau/2|0)\Phi(0)=\Phi(\tau/2)\exp(iA\tau/2)$$

[where each column vector of $\Phi(0)$ is uniquely determined to within a phase], therefore

$$\Phi^*(\tau/2)=\Phi(\tau/2) \quad (\text{Property 1}) \quad (31)$$

provided that $\Phi(0)$ is real (which we will now prove).

The second symmetry property is obtained through Eq. (25) by replacing C by $U(\tau|0)$ from Eq. (26), multiplying the equation on the right by $\Phi(0)$, and replacing the propagation expression $U(\tau|0)\Phi(0)$ by its propagated form $\Phi(\tau)\exp(iA\tau)$ to finally obtain

$$U^*(\tau/2-t|0)\Phi(\tau)e^{iA\tau}=U(\tau/2+t|0)\Phi(0). \quad (32)$$

Evaluating this expression at $t=-\tau/2$ and taking the complex conjugate reveals that

$$U(\tau|0)\Phi^*(0)=\Phi^*(0)e^{iA\tau}. \quad (33)$$

But since $U(\tau|0)\Phi(0)=\Phi(0)\exp(iA\tau)$,

$$\Phi(0)=\Phi^*(0) \quad (\text{Property 2}). \quad (34)$$

The third property is an important symmetry about $\Phi(\tau/2)$. Taking the complex conjugate of both sides of Eq. (28) and using Property 1 leads to

$$\Phi^*(\tau/2-t)e^{iAt}=U(\tau/2+t|\tau/2)\Phi(\tau/2). \quad (35)$$

But, by Eq. (27) the RHS is equal to $\Phi(\tau/2+t)e^{iAt}$. Therefore,

$$\Phi^*(\tau/2-t)=\Phi(\tau/2+t) \quad (\text{Property 3}). \quad (36)$$

The above properties provide three computational aids. First, since $\Phi(0)$ is real valued, complex diagonalization is not required in the eigenvector equation (16). The equation can be simply separated into real and imaginary parts. Solution of the real equation yields $\Phi(0)$ and $\cos(2\pi M)$. Second, by the time symmetry of Eq. (36), it is only necessary to calculate $\Phi(t)$ over the first half of the optical cycle. The third concerns the Fourier components of $\Phi(t)$, which are used to determine long-time-average transition probabilities and are written here as an integral from 0 to τ :

$$\phi_{in}^m = \int_0^\tau \Phi_{in}(t)e^{im\omega t} dt. \quad (37)$$

By transforming t to $\tau/2-t$, substituting $\Phi(\tau/2-t)$ from Eq. (28), and replacing $U^*(\tau/2+t|\tau/2)$ by its conjugate equivalent [Eq. (20)] the expression for ϕ_{in}^m becomes

$$\begin{aligned}\phi_{\text{in}}^m &= - \int_{\tau/2}^{-\tau/2} [U(\tau/2-t | \tau/2)\Phi(\tau/2)]_{\text{in}} \exp[-i(\mu_n+m)\omega t] e^{im\omega\tau/2} dt \\ &\equiv - \int_{\tau/2}^{-\tau/2} b_{\text{in}}(-t) \exp[-i(\mu_n+m)\omega t] e^{im\omega\tau/2} dt.\end{aligned}\quad (38)$$

Since $\Phi(\tau/2)$ is real [Eq. (31)], $b(-t)_{\text{in}} = b^*(+t)_{\text{in}}$ by Eq. (20). Also, $\exp(\pm im\omega\tau/2) = (-1)^m$. Using these facts, the integral may be split at $t=0$, and with a few simple manipulations Eq. (38) becomes

$$\phi_{\text{in}}^m = \left[(-1)^m \int_0^{\tau/2} b_{\text{in}}(t) \exp[i(\mu_n+m)\omega t] dt \right]^* + \left[(-1)^m \int_0^{\tau/2} b_{\text{in}}(t) \exp[i(\mu_n+m)\omega t] dt \right]. \quad (39)$$

Now, since the two terms on the RHS are complex conjugates, ϕ_{in}^m must be real. Therefore, all Fourier coefficients must be real valued and any imaginary part will be an indication of numerical error in the determination of $\Phi(t)$.

IV. ENERGY AND THE PERIODIC HAMILTONIAN

For a time-dependent Hamiltonian $H(t)$, there are no discrete energies as there are for the time-independent Hamiltonian of Eq. (7); therefore, the energies have a width and uncertainty associated with their measurement. The most practical approach, then, is to discuss the energy in terms of the discrete spectrum of some relevant operator. The operator \mathcal{H} , having eigenvectors Φ and FE as eigenvalues, is a natural choice for discussing the energy distribution of the molecular states while the field is on. \mathcal{H} was introduced by Samba¹⁵ as an extended Hilbert-space Hamiltonian which includes not only the configuration (R) but also time (T) in the function space ($R \oplus T$). The most important aspect of this concise mathematical formalism is that it relates a time-transition operator to the FE, as shown below. Also, within this space the mean energies, which were defined by Fainshtein, Manakov, and Rapoport¹⁶ as a natural consequence of evaluating the bracket of $H(t)$, provide a measure of the time-independent contribution to the energy.

Although the formalism of the configuration-time $R \oplus T$ space is attractive, its use limits the analysis to the range of only an optical cycle by the nature of the time integral of the new space [Eq. (41)]. However, the $R \oplus T$ formalism, which naturally defines and describes Floquet-state properties (such as the mean energy), suggests that these properties might appear in the time averages of the normal (R) Hilbert space where we determine the molecular-state dynamics and formulate the energy analysis.

To help understand the nature of mean energies, we present the salient points of the $R \oplus T$ Hilbert-

space formalism and its application to $H(t)$, as well as its relation to Shirley's H_F matrix. We will show how the FE's are correlated with the molecular energies, and later, how they are intimately related to the mean energies. Furthermore, it will be shown that the mean energy retains the same meaning when applied to the solutions derived by Shirley¹¹ or by Leasure and Wyatt¹⁹; the mean energy also serves as a comparative measure of the accuracy of $\Phi(t)$ calculations. Finally, we will show the unique character that mean energies and FE's play in the molecular-state energy analysis.

A. Floquet solutions in $R \oplus T$ Hilbert space

The formal development of the space-extended Hamiltonian \mathcal{H} begins by substituting the Floquet states $f_i(t)$ [where $f_i(t)$ and $\phi_i \exp(-i\mu_i\omega t)$ are the column vectors of $F(t)$ in Eq. (9)] into the Schrödinger equation to obtain

$$\mathcal{H}\phi_i(t) = \hbar\omega\mu_i\phi_i(t); \quad \mathcal{H} \equiv \left[H(t) - i\hbar \frac{\partial}{\partial t} \right]. \quad (40)$$

For the operator \mathcal{H} , Samba¹⁵ introduced the composite Hilbert space $R \oplus T$ of square-integrable functions $\{g(r), h(r), \dots\}$ on configuration space, with the inner product

$$\langle g(\vec{r}) | h(\vec{r}) \rangle \equiv \int_{-\infty}^{\infty} g^* h d\vec{r},$$

and square-integrable functions $\{a(t), b(t), \dots\}$ on time space, with the inner product

$$[a(t), b(t)] \equiv 1/\tau \int_{-\tau/2}^{\tau/2} a^* b dt.$$

Any function in the composite space may be formed from the direct product of an orthonormal basis function in each space. As a consequence, the inner product of an operator \mathcal{O} ,

$$\frac{1}{\tau} \int_{-\tau/2}^{\tau/2} dt \langle \phi_i(t) | \mathcal{O} | \phi_i(t) \rangle \equiv \langle \langle \phi_i | \mathcal{O} | \phi_i \rangle \rangle, \quad (41)$$

defines the mean value of the operator for the Floquet vector ϕ_i . Sambe further defined the time-transition operator $\mathcal{O}_{n\tau}$ which displaces the Floquet states in increments of τ :

$$\mathcal{O}_{n\tau} f_i(t+n\tau) = f_i(t) \quad (n=0, \pm 1, \pm 2, \dots) \quad (42)$$

Also, $\mathcal{O}_{n\tau}$ commutes with \mathcal{H} and has the property

$$\mathcal{O}_{n\tau} f_i(t) = e^{in\mu_i \omega \tau} f_i(t), \quad (43)$$

thereby forming an Abelian symmetry group of \mathcal{H} having one-dimensional irreducible representations involving the FCE. The time space may therefore be conveniently spanned by

$$e^{in\omega t} \quad (n=0, \pm 1, \pm 2, \dots) \quad (44)$$

and configuration space by some appropriate vector basis (e.g., the molecular states). The FCE's (or FE's) characterize the irreducible representations of the time-transition operator $\mathcal{O}_{n\tau}$.

Just as the periodic behavior of $\Phi(t)$ in $R \oplus T$ space suggests an expansion of the time dependence by the Fourier representation (functions) of Eq. (44), the same periodicity permits the Fourier expansion of both

$$H_{\text{in}}(t) = \sum_{m=-\infty}^{\infty} H_{\text{in}}^m e^{i\omega m t}$$

and

$$\phi_{\text{in}}(t) = \sum_{m=-\infty}^{\infty} \phi_{\text{in}}^m e^{i\omega m t}$$

and the creation of Shirley's "infinite Hamiltonian" H_F and the eigenvalue equation

$$\sum_{nl} \{H_F\}_{im, nl} \phi_{nl}^l = \hbar\omega \mu_l \phi_{il}^m; \quad (45)$$

$$\{H_F\}_{im, nl} \equiv H_{\text{in}}^{m-l} + m\hbar\omega \delta_{in} \delta_{lm}.$$

Again, $|i\rangle |m\rangle \equiv |im\rangle$, where $|i\rangle$ are the molecular eigenvectors of H_0 and $|m\rangle$ are the Fourier vectors, such that $\langle t | m \rangle = \exp(i\omega m t)$.

The rearrangement of the Schrödinger equation to create H_F in Eq. (45) is the same rearrangement used to create \mathcal{H} in Eq. (40) and the resulting eigenvector equation (45) is the same eigenvector equation of \mathcal{H} in the Fourier representation.

B. Floquet characteristic value correlation with molecular energy

The values μ_i are determined using an exponential, $\exp(-iM2\pi)$, in the eigenvalue equation (16)

for $\Phi(0)$. Therefore, each μ_i has multiple values:

$$\mu_i = {}^1\mu_i + n_i, \quad n_i = 0, \pm 1, \pm 2, \dots \quad (46)$$

where $0 \leq {}^1\mu_i < 1$. If for all μ_i , the n 's are made zero, the corresponding diagonal matrix 1M of all μ 's is said to belong to the first zone, etc. By redefining zones with a factor of $\hbar\omega$,

$$\hbar\omega \mu_i = \hbar\omega {}^1\mu_i + \hbar\omega n_i \equiv \{\Gamma\}_i, \quad (47)$$

the Γ matrix has the units of energy and is appropriately called the Floquet energy matrix. (If atomic units are used the FCE values are identical to the FE.) The restriction of Γ to the first zone is suggested by the mean energy definition in $R \oplus T$ space; but the confinement to the first zone is by no means a necessity for the $U\tau$ approach in R space. A general correlation of the γ_i with the molecular energies and wave functions upon adiabatic switching has been investigated elsewhere.^{14,15,19,23} However, for low and intermediate ranges of intensity, the physical significance of γ_i becomes apparent when more than one zone is used to define Γ . One may establish a one-to-one correlation to each molecular energy E_i , simply by adding n units of $\hbar\omega$ to all ${}^1\gamma$ to determine the closest $(n_i\hbar\omega + {}^1\gamma_i)$ to each molecular energy. The values of n will range from zero to n_f , where $(n_f - 1)\hbar\omega < E^{\text{max}} < n_f\hbar\omega$, and E^{max} is the maximum molecular-state energy. Ambiguity in assignment does occur for pairs of ${}^1\gamma_i$ at near-resonance frequencies and/or high intensities, but an assignment may be ascertained by following the correlation through lower intensities and nonresonant frequencies.

With the extended energy zone the correlation

$$E_i \simeq {}^1\gamma_i + n_i\hbar\omega \equiv E\gamma_i \quad (48)$$

can be made. This enhances the physical insight. In the limit of low- or no-field intensity, $H(t)$ approaches H_0 for which

$$U(t|0)\chi_i = e^{-iE_i t/\hbar} \chi_i;$$

where

$$H_0\chi_i = E_i\chi_i. \quad (49)$$

Also, the Floquet vector ϕ_i is propagated with a similar form

$$U(t|0)\phi_i(0) = e^{-i\gamma_i t/\hbar} \phi_i(t). \quad (50)$$

When ${}^E\Gamma$ is used, the limiting process reveals that $\exp(-iE\gamma_i t/\hbar)$ becomes the molecular-state propagator $\exp(-iE_i t/\hbar)$; $\phi_i(t)$ becomes stationary and approaches χ_i . It is evident that the dominant term in the Fourier expansion of $\phi_i(t)$ [Eq. (14)] is $\phi_{ii}^{m=0}$

in the zero-field limit. So, in general,

$$|\phi_{ii}^{m=0}| > |\phi_{ii}^{m \neq 0}| \quad \text{and} \quad |\phi_{in}^{m=0}| > |\phi_{in}^{m \neq 0}| \quad (51)$$

for low intensities and nonresonant frequencies.

When ω is adjusted to a resonance value, these conditions no longer hold and different (mixing) conditions determine the resonant single and multiphoton dynamics. The difference between E_i and the correlated γ_i , and the relative size of the $\Phi(0)$ matrix elements provide an indication of the molecular-state interaction.

C. Mean energy

Energy is not a conserved quantity for the explicitly time-dependent Hamiltonian. However, as a natural consequence of the space extended $R \oplus T$ formalism and Eq. (41), a mean energy¹⁶ $\langle\langle H_i \rangle\rangle$ is determined by the time average over one optical cycle of the bracket $\langle \phi_i | H(t) | \phi_i \rangle$ for all γ_i in zone 1:

$$\begin{aligned} \langle\langle H_i \rangle\rangle &= \langle\langle {}^1\phi_i | H(t) | {}^1\phi_i \rangle\rangle \\ &= {}^1\gamma_i + \langle\langle {}^1\phi_i | i\hbar \frac{\partial}{\partial t} | {}^1\phi_i \rangle\rangle \\ &= \sum_{m=-\infty}^{\infty} ({}^1\gamma_i - \hbar m \omega) \sum_n |{}^1\phi_{ni}^m|^2, \end{aligned} \quad (52)$$

where, in general, ${}^n\phi_i$ and ${}^n\phi_{ji}^m$ are determined by the zone of γ_i in the expression for f_i . When all γ_i are within the first, second, . . . or n th zone each Floquet state f_i (and therefore ${}^n\phi_i$) will be written as

$${}^1\phi_i(t) \exp[-i({}^1\gamma_i)t/\hbar] = {}^2\phi_i(t) \exp[-i({}^2\gamma_i)t/\hbar] = \dots \quad (\text{or}) \quad {}^n\phi_i(t) \exp[-i({}^n\gamma_i)t/\hbar], \quad (53)$$

respectively; and those f_i having γ_i 's correlated to the molecular-state energies by

$${}^E\phi_i(t) \exp[-i({}^E\gamma_i)t/\hbar]. \quad (54)$$

In Eq. (52) we see the FE, or the quasienergy, as a partial contribution to the average energy of ϕ_i . Equally important for the (average) energy expression is the contribution from the Fourier terms of $\phi_i(t)$.

We will now prove that the optical-cycle average in configuration space of $H(t)$ over the Floquet state f_i is equivalent to the mean energy for the Floquet ϕ_i vector, regardless of the zone(s) used. In configuration space this average H_i is defined by

$$\bar{H}_i \equiv 1/\tau \int_{-\tau/2}^{\tau/2} \langle f_i | H(t) | f_i \rangle. \quad (55)$$

By the Schrödinger equation the Hamiltonian may be replaced with the time operator $i\hbar\partial/\partial t$. By using the energy zone, Eq. (55) then becomes

$${}^E\bar{H}_i = 1/\tau \int_{-\tau/2}^{\tau/2} \exp[i({}^E\gamma_i)t/\hbar] \left\langle {}^E\phi_i \left| i\hbar \frac{\partial}{\partial t} \right| {}^E\phi_i \right\rangle \exp[-i({}^E\gamma_i)t/\hbar]. \quad (56)$$

By taking the partial derivative and replacing $|{}^E\phi_i(t)\rangle$ by its Fourier expansion $[\sum_m |{}^E\phi_i^m\rangle \exp(im\omega t)]$, Eq. (56) becomes

$${}^E\bar{H}_i = {}^E\gamma_i + \sum_m (-m\hbar\omega) \langle {}^E\phi_i^m | {}^E\phi_i^m \rangle, \quad (57)$$

where the superscript E designates that the energy zone was used.

Assuming that $({}^E\gamma_i + n_i\hbar\omega) = {}^1\gamma_i$, the elements of ϕ_i for the m th Fourier component in Eqs. (52) and (57) are related by Eq. (53):

$${}^E\phi_{ji}^m = {}^1\phi_{ji}^{m-n}. \quad (58)$$

Now, returning to Fainshtein's mean energy expression in Eq. (52), the Fourier expansion of the second equality,

$$\begin{aligned}
\langle \langle {}^1H_i \rangle \rangle &= 1/\tau \int_{-\tau/2}^{\tau/2} \left\langle {}^1\phi_i \left| \mathcal{H} + i\hbar \frac{\partial}{\partial t} \right| {}^1\phi_i \right\rangle \\
&= {}^1\gamma_i + 1/\tau \int_{-\tau/2}^{\tau/2} \sum_{m=-\infty}^{\infty} \sum_{m'=-\infty}^{\infty} e^{im\omega t} \left\langle {}^1\phi_i^m \left| i\hbar \frac{\partial}{\partial t} \right| {}^1\phi_i^{m'} \right\rangle e^{-im'\omega t}, \tag{59}
\end{aligned}$$

becomes, upon using Eq. (58) and the zone relation,

$$\langle \langle {}^1H_i \rangle \rangle = E\gamma_i + n\hbar\omega + \sum_{m=-\infty}^{\infty} (-m\hbar\omega) \sum_{k=-\infty}^{\infty} E\phi_{ki}^m - n E\phi_{ki}^{m-n},$$

and by combining the second and third terms, redefining the index, and using vector notation again

$$\langle \langle {}^1H_i \rangle \rangle = E\gamma_i + \sum_{m=-\infty}^{\infty} (-m\omega\hbar) \langle E\phi_i^m | E\phi_i^m \rangle. \tag{60}$$

Since Eqs. (57) and (60) are equivalent, the mean of the Hamiltonian $H(t)$ for the Floquet vector ${}^E\phi_i$ in $R \oplus T$ space is the same as the Hamiltonian average in R space over the Floquet States. Also, since any zone could have been used in Eq. (56), the equivalence of Eqs. (52) and (60) states that the mean energy is independent of the particular zone(s) to which γ_i is assigned.

D. Mean energy and the molecular-state energy

We define the energy for the molecular state $\chi_i(t)$ as the expectation value of the time-dependent Hamiltonian $H(t)$:

$$\langle H_i(t) \rangle = \langle \chi_i(t) | H(t) | \chi_i(t) \rangle. \tag{61}$$

Floquet theory provides insight into the time dependence of the ‘‘molecular-state’’ energies: When $\langle H_i(t) \rangle$ is expanded in the Floquet states, the resulting expression has a constant term as well as time-dependent terms which are related to single and multiphoton resonances. The constant term is just a simple sum of all the mean energies weighted by the square of corresponding $\Phi^\dagger(0)$ elements.

The evolution of $\phi_j(t)$ is linearly related through Eq. (27) to the $\chi_i(t)$ [the columns of the $U(t|0)$ matrix] by $\Phi(0)$. By the unitarity of $\Phi(t)$ and Property 2, the evolution of the molecular state $\chi_i(t)$ is

$$|\chi_i(t)\rangle = \sum_j \phi_{ij}(0) |f_j(t)\rangle. \tag{62}$$

By replacing $|\chi_i(t)\rangle$ in Eq. (61) by the RHS of Eq. (62) and expressing $H(t)$ in terms of the operator \mathcal{H} , Eq. (61) becomes

$$\langle H_i(t) \rangle = \sum_{ij} \phi_{ik}(0) \phi_{ij}(0) \left\langle f_i(t) \left| \mathcal{H} + i\hbar \frac{\partial}{\partial t} \right| f_j(t) \right\rangle, \tag{63}$$

or in terms of $|\phi_i(t)\rangle$,

$$\langle H_i(t) \rangle = \sum_k \phi_{ik}^2(0) \gamma_k + i\hbar \sum_{ij} \phi_{ik}(0) \phi_{ij}(0) \exp[-i(\gamma_i - \gamma_j)t/\hbar] \left\langle \phi_i(t) \left| \frac{\partial}{\partial t} \right| \phi_j(t) \right\rangle. \tag{64}$$

Substituting $|\phi_n(t)\rangle$ and its adjoint with their Fourier expansions, differentiating, replacing the brackets by their component form, and finally, grouping the time-dependent and dependent terms leads to

$$\begin{aligned}
\langle H_i(t) \rangle &= \sum_j \phi_{ij}^2(0) \bar{H}_j - \sum_j \phi_{ij}^2(0) \sum_{\substack{k \neq m \\ km}} m\hbar\omega \sum_n \phi_{nj}^k \phi_{nj}^m \exp[-i(k-m)\omega t] \\
&\quad - \sum_{ij}^{i \neq j} \phi_{ik}(0) \phi_{ij}(0) \sum_m m\hbar\omega \sum_n \phi_{ni}^m \phi_{nj}^m \exp[-i(\mu_j - \mu_i)\omega t] \\
&\quad - \sum_{ij}^{i \neq j} \phi_{ik}(0) \phi_{ij}(0) \sum_{\substack{k \neq m \\ km}} m\hbar\omega \sum_n \phi_{ni}^k \phi_{nj}^m \exp[-i(\mu_j - \mu_i + k - m)\omega t] \tag{65}
\end{aligned}$$

(k and m sums are from $-\infty$ to ∞ .) The constant term is simply the sum of a distribution of mean energies, with weights determined by the initial probability distribution of the molecular state χ_i in the Floquet states. In relation to the field frequency ω , the second term has equal or higher oscillating factors. The third has slowly oscillating terms near resonances [i.e., when μ_j is near μ_i and the corresponding $\Phi(0)$ components are large]. The fourth term might be thought of as a molecule-field interaction term. Near resonance, when the Floquet characteristic exponent difference $\mu_j - \mu_i$ is close to the fieldlike Fourier difference $k - m$, long-time oscillations occur. We see then, that the center of the (field on) energy distribution of the state χ_i is given by the constant term and that its width is determined by the slowly oscillating contributions of Eq. (65).

V. MAGNUS APPROXIMATION FOR $U(t | 0)$

There are basically two formal approaches to determine analytic approximations to the propagator for a time-dependent Hamiltonian. One approach is through the integral solution

$$U(t | t_0) = \mathcal{D} \exp[-i/\hbar \int_{t_0}^t H(t') dt'], \quad (66)$$

which invokes the formidable Dyson time-ordering operator.²⁴ The other is by the differential solution, Eq. (4).

$$A_1(t, t_0) = \frac{-i}{\hbar} \int_{t_0}^t dt_1 H(t_1), \quad A_2(t, t_0) = \frac{1}{2\hbar^2} \int_{t_0}^t dt_2 \int_{t_0}^{t_2} dt_1 [H(t_1), H(t_2)], \dots \quad (70)$$

Since there are multibracket commutators in Eq. (69) a large number of different permutations in the arguments are possible and, therefore, the correct form of the truncated series may vary among authors. Also, the second approximation leads to non-separable multidimensional integrals, with limits which present somewhat of a challenge to keep record of in the higher-order expressions. Derivations of these expressions have been given by Pechukas and Light,²⁵ Robinson,²⁶ and Magnus.²¹ In Ref. 25 we have found the third- and fourth-order integral limits to be incorrect; in the iterative integrations the proper lower-order iteration limits were replaced by higher-order limits. This error, incorrect integral limits in the recursion expansion, could explain the failure to obtain enhanced accuracy or convergence with this third-order expression in other works, including our own.^{7,27} For completeness

The Magnus²¹ formulation determines the propagator in an exponential form, $U(t | t_0) = \exp[A(t, t_0)]$, through the differential equation, i.e.,

$$i\hbar \frac{\partial (e^{A(t, t_0)})}{\partial t} = H(t) e^{A(t, t_0)}, \quad (67)$$

where $A(t, t_0)$ is given as an infinite series:

$$A(t, t_0) = A_1(t, t_0) + A_2(t, t_0) + \dots \quad (68)$$

The time dependence of A as well as H will now be suppressed for convenience, except where clarity is needed.

The truncation of the series at A_n is the n th-order Magnus approximation. Each A_i is anti-Hermitian, thereby preserving the unitary nature of e^A at any order. In the formation of the n th-order analytic expression there are two approximations used. After the RHS exponential in Eq. (67) is expanded

$$i\hbar \frac{\partial A}{\partial t} = H - \frac{[A, H]}{2} + \frac{[A[A, H]]}{12} + \dots; \quad (69)$$

the first approximation is made by a truncation of the series. The second approximation is the iterative integral of the truncated equation, which for Hamiltonians of the form $\hat{H}(t) = \sum_j \hat{O}_j g_j(t)$, where \hat{O}_j is an arbitrary time-independent operator and $g_j(t)$ is solely a function of time, can be performed simply by successive integrations. This leads to the expressions

the A_1 through A_5 terms of the Magnus propagator for time-dependent Hamiltonians are listed in Table I. The number of integrals and commutators to evaluate clearly grows rapidly with successive orders of approximation.

The analytic form of A is determined by the time-dependent "picture" of the Hamiltonian. Equation (67) is the equation of motion in the Schrödinger picture; its operators will now be superscripted for clarity by the letter s . The transformation from the Schrödinger picture to the interaction picture allows the dynamics to follow the equation

$$i\hbar \frac{\partial U^I(t | t_0)}{\partial t} = H^I(t) U^I(t | t_0), \quad (71)$$

where the interaction Hamiltonian $H^I(t)$ is

$$H^I(t) = e^{+iEt/\hbar} V \cos(\omega t) e^{-iEt/\hbar} \quad (72)$$

TABLE I. First- through fifth-order A operators for the Magnus approximation, $\exp(A) \cong \exp(A_1 + A_2 + A_3 + A_4 + A_5)$, for the propagator $U(t | t_0)$. These expressions may be applied to any time-dependent Hamiltonian.^a

$$\begin{aligned}
 A_1 \hbar^1 &= (-i) \{^1 H_1\} \\
 A_2 \hbar^2 &= (1/2) \{^2 H_1, H_2\} \\
 A_3 \hbar^3 &= (i/4) \{^3 H_1, H_2\} H_3 + (1/3) \{^3 H_1, H_2, H_3\} \\
 A_4 \hbar^4 &= -(1/8) \{^4 H_1, H_2\} H_3 H_4 + (1/3) \{^4 H_1, H_2, H_3\} H_4 \\
 &\quad + (1/3) \{^4 H_1, H_2, H_3, H_4\} + (1/3) \{^4 H_1, H_2\} H_3 H_4 \\
 A_5 \hbar^5 &= -(i/16) \{^5 H_1, H_2\} H_3 H_4 H_5 + (1/3) \{^5 H_1, H_2, H_3\} H_4 H_5 \\
 &\quad + (1/3) \{^5 H_1, H_2, H_3, H_4\} H_5 + (1/3) \{^5 H_1, H_2, H_3, H_4, H_5\} \\
 &\quad + (1/3) \{^5 H_1, H_2, H_3\} H_4 H_5 + (1/9) \{^5 H_1, H_2, H_3, H_4\} H_5 \\
 &\quad + (1/3) \{^5 H_1, H_2, H_3\} H_4 H_5 + (1/3) \{^5 H_1, H_2, H_3, H_4, H_5\} \\
 &\quad + (1/9) \{^5 H_1, H_2, H_3, H_4\} H_5 - (1/45) \{^5 H_1, H_2, H_3, H_4, H_5\}
 \end{aligned}$$

^aThe integral representation $\int_{t_0}^t dt_n \cdots \int_{t_0}^{t_{i-1}} dt_i \cdots \int_{t_0}^{t_2} dt_2 \int_{t_0}^{t_1} dt_1$, where the sequence of integration is performed in order from right to left, has been replaced by ${}^t \cdots {}^{t_i} \cdots {}^{t_2} {}^{t_1}$. Also, $H(t_i)$ is represented by H_i .

for the sinusoidal Hamiltonian $H(t)$. The Schrödinger and interaction-picture propagators are related by

$$U^S(t | t_0) = e^{-iEt/\hbar} U^I(t | t_0) e^{+iEt_0/\hbar}, \quad (73)$$

and by the similarity of Eqs. (68) and (72) the formal expressions in Table I apply to U^S when H^S is used, or to U^I when H^I is used.

The Schrödinger picture Hamiltonian has a much simpler, time-dependent form than the interaction-picture Hamiltonian H^I [compare Eqs. (1) and (72)]. However, the additional operator (E) makes it seem formidable to even write out the commutator expressions (in Table I) for third order and higher A 's. But because E is diagonal, simplification readily occurs. The first- through fourth-order A^S matrix elements are given in Table II. These expressions are relatively simple compared to the corresponding interaction-picture elements. The computation of

even a fourth-order Schrödinger picture matrix element takes less than the corresponding third-order interaction-picture element.

Another feature of the Schrödinger picture Magnus approximation for A is the form of each element in the series. The time-dependent factor in each A_r expression (see Table II) always appears with products (ωt) and has no other ω dependence, while the time-dependent factor has a simple ω^{-r} dependence. For an optical cycle the range of ωt (0 to 2π) is constant and also frequency independent [because of the boundary condition $\Phi(t + \tau) = \Phi(t)$]. So, in a spectral analysis, using any arbitrarily chosen set of points within this range, the computationally time-consuming factor of each A_r term need only be calculated once for this set of points regardless of the frequency. Also, the ω^{-r} terms of the time-independent factors show that the relative size of ω to successive expansion matrix is important for convergence.

TABLE II. First- through fourth-order terms of the Magnus exponential A matrix, evaluated for the Schrödinger picture (sinusoidal) Hamiltonian $[E + V \cos(\omega t)]$.^a For the following equations $U(t | 0) = \exp(A) \cong \exp(A_1 + A_2 + A_3 + A_4)$ and $\hbar = 1$.

$$\begin{aligned}
 \{A_1\}_{in} i\omega^1 &= E_i \delta_{in} [T] + V_{in} [S(T)] \\
 \{A_2\}_{in} i\omega^2 &= iV_{in} \{E_i - E_n\} \{2[C(T) - 1] + TS(T)\} / 2 \\
 \{A_3\}_{in} i\omega^3 &= V_{in} \{E_i - E_n\}^2 \{(12 - T^2)S(T) - 6T[C(T) + 1]\} / 12 \\
 &\quad + \sum_j V_{ij} V_{jn} \{E_i + E_n - 2E_j\} \{12S(T) - 3S(2T) - T[7 - C(2T)]\} / 24 \\
 \{A_4\}_{in} i\omega^4 &= iV_{in} \{E_i - E_n\}^3 \{24[C(T) - 1] + 12TS(T) - 2T^2[C(T) - 1]\} / 24 \\
 &\quad + i \sum_j V_{ij} V_{jn} \{E_i - E_n\} \{E_i + E_n - 2E_j\} \{-18 + 4C(T) + 14C(2T) + 16TS(T) \\
 &\quad + 10TS(2T) - 2T^2[C(2T) - 1]\} / 96 \\
 &\quad + i \sum_{jk} V_{ij} V_{jk} V_{kn} \{E_i - 3E_j + 3E_k - E_n\} \{44 - 33C(T) - 12C(2T) + C(3T) - 4TS(T)\} / 288
 \end{aligned}$$

^aThe product $\omega t = T$. The $\{E_i\}$ are the eigenenergies corresponding to the molecular states $\{|i\rangle\}$. The element $V_{in} = \vec{\epsilon} \cdot \vec{\mu}_{in}$, where $\vec{\epsilon}$ is the electric field vector, and $\vec{\mu}_{in}$ is the $i-n$ molecule-state bracket of the molecular dipole. $C(T)$ and $S(T)$ are, respectively, the cosine and sine functions of the argument (T).

In the interaction picture, the commutator expansions of A^I in Table I are simpler than those of the Schrödinger picture. Also, under perturbative conditions (i.e., $|E_{ii}| \geq |V_{in}|$), the solution $U^I(t|0)$ will be free from highly oscillatory time dependence of the diagonal energies in the Schrödinger picture. With the more slowly oscillating propagator $U^I(t|0)$ fewer time steps are required for numerical integration of the equations of motion.

The interaction-picture matrix elements for A_r in the molecular eigenstate representation are listed in Table III. For clarity, the equations retain much of the form that is derived from the straightforward integration indicated in Table I. Note that each $\{A_r^I\}_{in}$ expression, unlike the corresponding Schrödinger term, is neither a simple function of time nor of ω (greek symbols have a ω^{-1} dependence).

Included in Sec. VI will be numerical comparison of calculations incorporating Magnus approximations with those based upon exact numerical integration techniques.

VI. APPLICATION OF FLOQUET ANALYSIS TO THE HF VIBROTOR

In this section, using the $U\tau$ Floquet formalism, both dynamic and time-averaged properties for one- and two-photon excitations of the HF rotor in intense IR classical fields are determined. The details of the interaction and the numerical methods are described first, followed by a discussion of the convergence in the basis set and integration step size. Next, the symmetry of the Schrödinger picture fundamental propagator and $\Phi(t)$ are compared at resonance conditions. Then, time-averaged one-photon and two-photon transition probabilities are compared at different field intensities and frequencies. Their spectral widths and shifts at different intensities are determined and the one-photon values are shown to agree with two-state perturbation calculations. The time dependence of states in resonance with the field is explored by survival plots²⁸ whose predominant periodic behavior is predicted by a two-state approximation for the Rabi frequency. Next, we show how the resonance frequency (and its shift with intensity) may be determined from only the correlated Floquet characteristic exponents. Finally, the effects of competition between one- and two-photon absorption is shown to occur in HF (as well as other molecules) and to be a measurable phenomena.

A. Numerical methods

For the HF rotor, the direct product of Morse oscillator and spherical harmonics are used as the basis. The molecular constants and the matrix expressions coupling the molecular states to the field are given in our previous work,⁷ as well as the Floquet analytic long-time—average probability expression. However, the following modifications in the numerical methods were made. Accurate matrix elements of the vibrational displacement bracket, $\langle \chi_i | r - r_e | \chi_j \rangle$, were determined by using analytic expressions for the Morse wave functions and integrating the expression on each interval by analytic integration of a quintic polynomial interpolation. We also used slightly different physical constants: $2.194\,746 \times 10^5$ cm⁻¹/hartree, $1.882\,84 \times 10^3$ atomic units of mass/amu. We mention this latter change because it has shifted the molecular energies and the HF spectra as much as 10 cm⁻¹. Also, a much faster and more accurate integrator²² (Bulirsch-Stoer²⁹) was incorporated to integrate the equations of motion across the first optical cycle.

Even though the numerical “machinery” may take a long time to assemble, the computational procedure can be separated into both conceptual and developmental stages. In general, the procedure is to first determine the molecular states and energies, followed by the construction of the interaction matrix in the molecular-state basis. Then $U(\tau|0)$ is calculated in one step by the Magnus approximation or by numerically integrating the equations of motion over the first (1/2) optical cycle. Next the eigenvalue equation (16) is solved for $\Phi(0)$ and the FCE. At this point the correlation of the FE may be made with the molecular states. The propagator values $U(t_i|0)$ for n points over the first optical cycle are either calculated by the Magnus approximation or recalled from the stored numerical integration results and used in the inverted form of Eq. (17) to obtain $\Phi(t)$. The Fourier expansion coefficients of each $\Phi_{in}(t)$ are determined through a (fast) Fourier transformation (using 2^N equally spaced steps within the first optical cycle). Long-time—average probabilities and dynamics of the molecular states for times greater than one optical cycle are then calculated with $\Phi(t)$, the FE, and the Fourier coefficients.

Transitions are labeled $(\nu_f, J_f \leftarrow \nu_i, J_i)$, where ν is the Morse vibrator number and J the rotor number; i and f indicate the initial and final states, respectively. All calculations have been made with the angular momentum projection number m equal to

TABLE III. (a) First- through third-order terms of the Magnus exponential A matrix, evaluated for the interaction-picture (sinusoidal) Hamiltonian $[e^{iE_j t/\hbar} V e^{-iE_j t/\hbar} \cos(\omega t)]^a$. For the following equations $U(t|0) = \exp(A) \equiv \exp(A_1 + A_2 + A_3)$ and $\hbar = 1$. (b) $i-n$ matrix element of A_3 is the sum of the A_3^a and A_3^b terms. $S_{ijk} = V_{ij} V_{jk}$ and $S_{ijkn} = V_{ij} V_{jk} V_{kn}$. For the A_1 and A_2 terms $\alpha = (E_i - E_j)/\omega$ and $\beta = (E_j - E_k)/\omega$. The values of α , β , and γ for A_3 terms are determined by $P_r(\alpha\beta\gamma)$ as listed below.

$$\begin{aligned}
 \{A_1\}_{ij} &= -V_{ij} \left[\frac{e^{i(\alpha+1)T}-1}{(\alpha+1)} + \frac{e^{i(\alpha-1)T}-1}{(\alpha-1)} \right] / 2\omega \\
 \{A_2\}_{ik} &= -\sum_j S_{ijk} \left[\frac{1}{(\alpha+1)} - \frac{1}{(\beta+1)} \right] \left[\frac{e^{i(\alpha+\beta+2)T}-1}{(\alpha+\beta+2)} + \frac{(e^{i(\alpha+\beta)T}-1)D}{(\alpha+1)(\beta-1)} \right] + \left[\frac{1}{(\alpha-1)} - \frac{1}{(\beta-1)} \right] \left[\frac{e^{i(\alpha+\beta-2)T}-1}{(\alpha+\beta-2)} + \frac{e^{i(\alpha+\beta)T}-1}{(\alpha+1)} D \right] \\
 &\quad - \left[\frac{1}{(\alpha+1)(\beta+1)} \right] (-e^{i(\alpha+1)T} + e^{i(\beta+1)T}) - \left[\frac{1}{(\alpha+1)(\beta-1)} \right] (-e^{i(\alpha+1)T} + e^{i(\beta-1)T}) \\
 &\quad - \left[\frac{1}{(\alpha-1)(\beta+1)} \right] (-e^{i(\alpha-1)T} + e^{i(\beta+1)T}) - \left[\frac{1}{(\alpha-1)(\beta-1)} \right] (-e^{i(\alpha-1)T} + e^{i(\beta-1)T}) - \left[\frac{1}{(\alpha+1)} + \frac{1}{(\alpha-1)} - \frac{1}{(\beta+1)} - \frac{1}{(\beta-1)} \right] \{iTZ\} / (8\omega^2)
 \end{aligned}
 \tag{a}$$

For $i=k$, $D=0$ and $Z=1$ otherwise $D=1/(\alpha+\beta)$ and $Z=0$.

$$\begin{aligned}
 \{A_3^a\}_{in} &= -\sum_{r=1}^6 P_r(\alpha\beta\gamma) M_r S_{ijkn} \left[\frac{1}{(\alpha+1)(\alpha+\beta+2)} \left[\frac{e^{i(\alpha+\beta+\gamma+3)T}-1}{(\alpha+\beta+\gamma+3)} + \frac{e^{i(\alpha+\beta+\gamma+1)T}-1}{(\alpha+\beta+\gamma+1)} \right] + \frac{1}{(\alpha-1)(\alpha+\beta-2)} \left[\frac{e^{i(\alpha+\beta+\gamma-3)T}-1}{(\alpha+\beta+\gamma-3)} + \frac{e^{i(\alpha+\beta+\gamma-1)T}-1}{(\alpha+\beta+\gamma-1)} \right] \right] \\
 &\quad + \frac{2\alpha B}{(\alpha^2-1)} \left[\frac{e^{i(\alpha+\beta+\gamma+1)T}-1}{(\alpha+\beta+\gamma+1)} + \frac{e^{i(\alpha+\beta+\gamma-1)T}-1}{(\alpha+\beta+\gamma-1)} \right] - \frac{2\alpha}{(\alpha^2-1)(\beta+1)} \left[\frac{e^{i(\beta+\gamma+2)T}-1}{(\beta+\gamma+2)} + \frac{e^{i(\beta+\gamma)T}-1}{(1/C)} \right] - \frac{2\alpha}{(\alpha^2-1)(\beta-1)} \\
 &\quad \times \left[\frac{e^{i(\beta+\gamma-2)T}-1}{(\beta+\gamma-2)} + \frac{e^{i(\beta+\gamma)T}-1}{(1/C)} \right] - \left[\frac{1}{(\alpha+1)(\alpha+\beta+2)} + \frac{1}{(\alpha-1)(\alpha+\beta-2)} + \frac{2\alpha C}{(\alpha^2-1)} - \frac{2\alpha}{(\alpha^2-1)(\beta-1)} \right] \\
 &\quad \times \left[\frac{e^{i(\gamma+1)T}-1}{(\gamma+1)} + \frac{e^{i(\gamma-1)T}-1}{(\gamma-1)} \right] / (32\omega^3)
 \end{aligned}$$

For $i=k$, $B=0$ otherwise $B = \frac{1}{(\alpha+\beta)}$.

For $j=n$, $C=0$ otherwise $C = \frac{1}{(\beta+\gamma)}$.

TABLE III. (Continued.)

$$\{A_3^i\}_{in} = - \sum_{r=1}^6 P_r(\alpha\beta\gamma) N_r S_{ijkn}$$

$$\times \left[\frac{1}{(\alpha+1)(\beta+1)} \left[\frac{e^{i(\alpha+\beta+\gamma+3)T-1}}{(\alpha+\beta+\gamma+3)} + \frac{e^{i(\alpha+\beta+\gamma+1)T-1}}{(\alpha+\beta+\gamma+1)} - \frac{e^{i(\alpha+\gamma+2)T-1}}{(\alpha+\gamma+2)} - \frac{e^{i(\beta+\gamma+2)T-1}}{(\beta+\gamma+2)} - F - G + H \right] \right.$$

$$+ \frac{1}{(\alpha+1)(\beta-1)} \left[\frac{e^{i(\alpha+\beta+\gamma+1)T-1}}{(\alpha+\beta+\gamma+1)} + \frac{e^{i(\alpha+\beta+\gamma-1)T-1}}{(\alpha+\beta+\gamma-1)} - \frac{e^{i(\alpha+\gamma+2)T-1}}{(\alpha+\gamma+2)} - \frac{e^{i(\beta+\gamma-2)T-1}}{(\beta+\gamma-2)} - F - G + H \right]$$

$$+ \frac{1}{(\alpha-1)(\beta+1)} \left[\frac{e^{i(\alpha+\beta+\gamma+1)T-1}}{(\alpha+\beta+\gamma+1)} + \frac{e^{i(\alpha+\beta+\gamma-1)T-1}}{(\alpha+\beta+\gamma-1)} - \frac{e^{i(\beta+\gamma+2)T-1}}{(\beta+\gamma+2)} - \frac{e^{i(\alpha+\gamma-2)T-1}}{(\alpha+\gamma-2)} - F - G + H \right]$$

$$+ \frac{1}{(\alpha-1)(\beta-1)} \left[\frac{e^{i(\alpha+\beta+\gamma-3)T-1}}{(\alpha+\beta+\gamma-3)} + \frac{e^{i(\alpha+\beta+\gamma-1)T-1}}{(\alpha+\beta+\gamma-1)} - \frac{e^{i(\alpha+\gamma-2)T-1}}{(\alpha+\gamma-2)} - \frac{e^{i(\beta+\gamma-2)T-1}}{(\beta+\gamma-2)} - F - G + H \right]$$

$$- I \left[\frac{1}{(\alpha+1)(\beta+1)} + \frac{1}{(\alpha+1)(\beta-1)} + \frac{1}{(\alpha-1)(\beta+1)} + \frac{1}{(\alpha-1)(\beta-1)} \right] iT \Big/ (96\omega^3),$$

where $H = \frac{e^{i(\gamma+1)T-1}}{(\gamma+1)} + \frac{e^{i(\gamma-1)T-1}}{(\gamma-1)}$.

For $k = j$ and $i = n$, or $k = n$ and $i = j$, $F = 0$ otherwise $F = \frac{e^{i(\alpha+\gamma)T-1}}{(\alpha+\gamma)}$.

For $j = n$, $G = 0$ otherwise $G = \frac{e^{i(\beta+\gamma)T-1}}{(\beta+\gamma)}$.

If $F = 0$ and $G \neq 0$ then $I = 0$; if $F = 0$ and $G = 0$ then $I = 2$ otherwise $I = 1$.

TABLE III. (Continued.)

r	$P_r(\alpha\beta\gamma)$			M_r	N_r
	α	β	γ		
		(b)			
1	$(E_i - E_j)/\omega$	$(E_j - E_k)/\omega$	$(E_k - E_n)/\omega$	1	1
2	$(E_i - E_j)/\omega$	$(E_k - E_n)/\omega$	$(E_j - E_k)/\omega$	0	-1
3	$(E_k - E_n)/\omega$	$(E_i - E_j)/\omega$	$(E_j - E_k)/\omega$	0	-1
4	$(E_j - E_k)/\omega$	$(E_i - E_j)/\omega$	$(E_k - E_n)/\omega$	-1	0
5	$(E_j - E_k)/\omega$	$(E_k - E_n)/\omega$	$(E_i - E_j)/\omega$	-1	0
6	$(E_k - E_n)/\omega$	$(E_j - E_k)/\omega$	$(E_i - E_j)/\omega$	1	1

zero. The choice of both the rotor and vibrator basis size, and the number of steps for numerical integration were determined, in part, by the computational time needed to perform the task. They were also chosen by the accuracy with which they represented the converged results. Since the Floquet energies and $\Phi(0)$ directly determine the dynamics, as opposed to the long-time-average probabilities, they are used as a criteria for convergence. Table IV shows the convergence in vibrator states for the one- and two-photon transitions, $(1,1 \leftarrow 0,0)$ and $(2,2 \leftarrow 0,0)$, respectively, having seven rotors in each vibrational manifold. Since the increment between the values of the four-, five- and six-vibrator state basis vary much less than the increment between the three- and four-vibrator basis, four vibrator states are used in the calculations of this section.

Table V shows that only four rotor states in each vibrator manifold are necessary to attain about the same degree of accuracy as the four-vibrator state basis. However, throughout this section, seven rotors in each manifold were used.

Because the fast Fourier method was used in the analysis it was necessary to numerically integrate with 2^N steps. This means the 64 steps would be necessary to obtain the next higher accuracy after a 32-step integration. However, for all intensities and frequencies we found it unnecessary to use 64 steps. Propagator elements of 64 steps generally changed by only 10^{-8} in magnitude at the most.

B. Symmetry of $\Phi(t)$

Figure 1 shows a plot of the complicated structure in the propagator element $U_{(11,00)}$ for the ground- $(0,0)$ to-resonant-state $(1,1)$ transition of HF over the first optical cycle, while Fig. 2 shows the symmetry (the three properties of Sec. III of the corresponding element of the correlated Floquet

periodic function $\Phi_{[11,00]}$. [Brackets indicate that $\phi(t)$ was determined using the energy correlation, as explained in Sec. IV.] Note that $\phi(t)$ is real valued at times 0, $\tau/2$, and τ . Also, the real component of $\phi(t)$ is symmetric about $\tau/2$ while the imaginary part is inverted. Another important property, not shown by these plots, is that the Fourier expansion coefficients of $\phi(t)$ are real; in all calculations the imaginary components of the largest coefficients were found to be the order of 10^{-13} .

In the plots of the $\Phi(t)$ elements which we have studied so far, the simple sinusoidal character found in Fig. 2 was prevalent, indicating (as also found in the numerical results), that the Fourier expansions of $\Phi(t)$ elements are dominated by just one or only a few terms. It is therefore reasonable to suspect that models which incorporate only the major components should be quite useful and accurate in representing the major time dependence of $\Phi(t)$.

C. One-photon transitions

A plot of the $(1,1 \leftarrow 0,0)$ one-photon long-time-average transition probability versus frequency is shown in Fig. 3. These results were obtained from the numerically integrated interaction-picture (NI) propagator. The "field-free" transition frequency is 0.018 249 09 a.u. As the field intensity is increased from 0.1 to 1.0 TW/cm², the one-photon resonance at 0.018 250 2 a.u. is blue shifted to 0.018 261 0 a.u.

According to the two-state perturbative formula of Shirley¹¹ the power broadening for the $(1,1 \leftarrow 0,0)$ transition is

$$\text{FWHM} = 2V_{11,00} . \quad (74)$$

The exact FWHM's were evaluated directly from Fig. 3. They are 0.754×10^{-4} and 0.234×10^{-3} a.u. (at 0.1 and 1.0 Tw/cm², respectively) and agree well with the perturbative predications of 0.752×10^{-4} and 0.238×10^{-3} a.u. This type of agreement is ex-

TABLE IV. Convergence in vibrator states. Floquet energies (FE) and the corresponding diagonal $\phi(0)$ elements are used as convergence criteria. Each vibrator manifold contains the lowest seven rotor states.

Number of vibrator states	One-photon resonances				Two-photon resonances			
	$\omega = 0.01824909$ (a.u.)	$I = 0.1$ TW/cm ²	$\omega = 0.01826100$ (a.u.)	$I = 1.0$ TW/cm ²	$\omega = 0.0179322$ (a.u.)	$I = 0.1$ TW/cm ²	$\omega = 0.01793405$ (a.u.)	$I = 1.0$ TW/cm ²
	FE(10 ²)	Floquet state $\phi(0)$	Floquet state [1,1]	Floquet state $\phi(0)$	FE(10 ²)	Floquet state $\phi(0)$	Floquet state [0,0]	Floquet state $\phi(0)$
3	0.93122940165	0.70879	2.75987329770	0.70924	0.92656321314	0.74364	2.76457451908	0.74798
4	0.93126421517	0.71494	2.75993100923	0.71592	0.92721983293	0.71550	2.76506611450	0.70553
5	0.93126421260	0.71494	2.75993100651	0.71592	0.92721977742	0.71551	2.76506606482	0.70554
6	0.93126421249	0.71494	2.75993100639	0.71592	0.92721977419	0.71551	2.76506606227	0.70554
	FE(10 ²)	Floquet state $\phi(0)$	Floquet state [1,1]	Floquet state $\phi(0)$	FE(10 ²)	Floquet state $\phi(0)$	Floquet state [1,1]	Floquet state $\phi(0)$
3	0.93293751324	0.82511	4.52972137782	0.82722	0.93165114089	0.78240	4.51981102137	0.80235
4	0.93284753188	0.71776	4.52972597848	0.71956	0.93089015180	0.68172	4.52031963879	0.69624
5	0.93284741475	0.71746	4.51977085056	0.71926	0.93089367189	0.68268	4.52032317308	0.69707
6	0.93284740924	0.71745	4.51977084459	0.71925	0.93089357751	0.68265	4.52032306820	0.69704

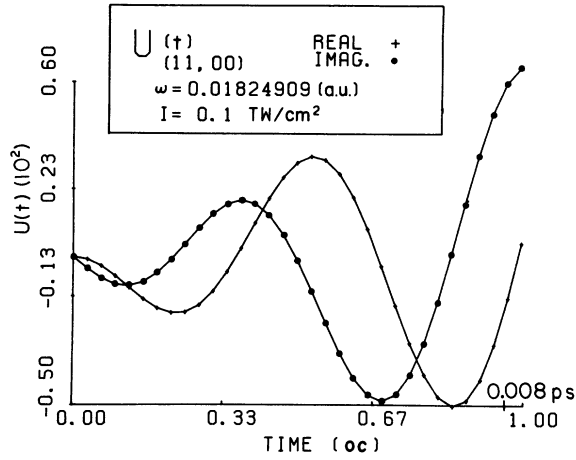


FIG. 1. Time dependence of the fundamental propagator for the HF vibrotor during the first optical cycle (0.008 33 ps) for the one-photon resonant transition ($\nu=1, J=1 \leftarrow \nu=0, J=0$). Field frequency $\omega=0.01824909$ (a.u.). Intensity $I=0.1$ TW/cm².

pected for isolated one-photon resonances. The two-state Rabi frequency and transition probability for the one-photon transition ($1,1 \leftarrow 0,0$) is given by the equation³⁰

$$P_{11,00}(t) = \sin^2(\nu t/2); \quad \nu = V_{11,00}/\hbar. \quad (75)$$

At 0.1 TW/cm² ($\omega_{\text{res}}=0.0182502$) and 1.0 TW/cm² ($\omega_{\text{res}}=0.0182610$) the Rabi formula predicts 485 and 153 optical cycles/Rabi cycle, respectively. The same values were obtained from

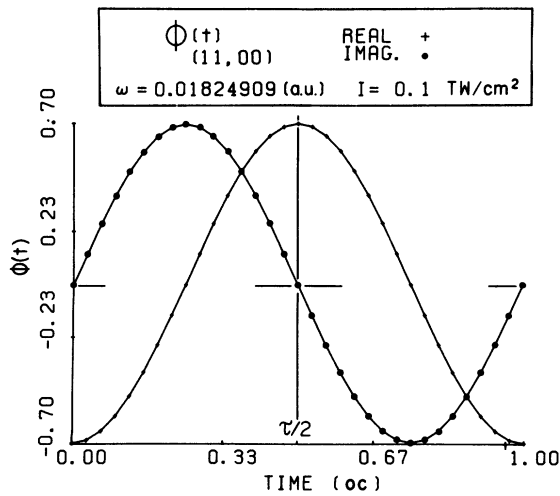


FIG. 2. Time dependence of the Floquet $\Phi_{[11,00]}$ element for the one-photon resonance ($\nu=1, J=1 \leftarrow \nu=0, J=0$). Field frequency $\omega=0.01824909$ (a.u.). Intensity $I=0.1$ TW/cm².

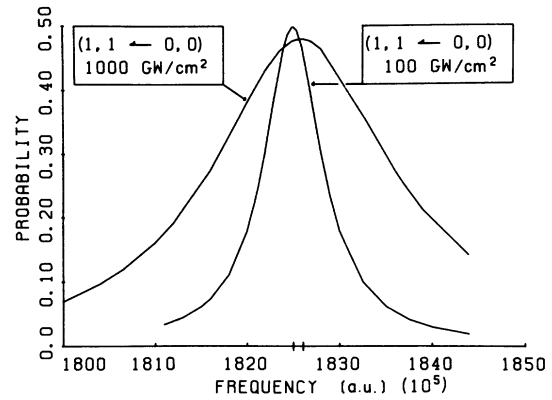


FIG. 3. One-photon absorption spectrum of HF for the resonant transition ($\nu=1, J=1 \leftarrow \nu=0, J=0$) at 0.1 and 1.0 TW/cm². Peak maxima are marked on the frequency axis; the field-free "maximum" is visually indistinguishable from the 0.1 TW/cm² maximum.

plots of the time-dependent transition probabilities, $|U_{11,00}|^2$. Figure 4 shows a plot of the transition probability at the frequency 0.01824909 a.u., only 1.2×10^{-6} away from the 0.1 TW/cm² resonance.

Even though the two-state Rabi and FWHM parameters predict well the resonant Rabi frequency and resonance width for the one-photon ($1,1 \leftarrow 0,0$) transitions, plots of transition probabilities near 1.0 TW/cm² show multistate effects. For example, Fig. 5 is a plot of the survival probability of state ($0,0$), that is, the probability for beginning in state

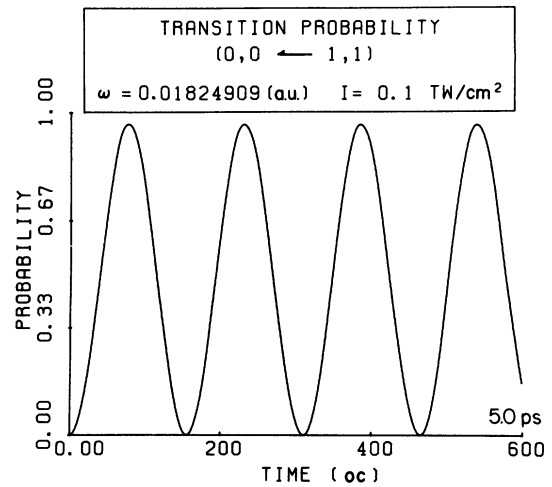


FIG. 4. Transition probability of the HF one-photon transition ($\nu=1, J=1 \leftarrow \nu=0, J=0$) for 600 oc (5.00 ps). Field frequency $\omega=0.01824909$. Intensity $I=1.0$ TW/cm².

TABLE V. Convergence in the rotor states. Floquet energies (FE) and the corresponding diagonal $\Phi(0)$ elements are used as convergence criteria. The lowest four vibrator manifolds were included in all calculations.

Number of rotor states	One-photon resonance							
	$\omega = 0.1824909$ (a.u.)		$I = 0.1$ TW/cm ²		$\omega = 0.018261$ (a.u.)			
	$\Phi(10^2)$	$\Phi(0)$	Floquet state	$\Phi(10^2)$	$\Phi(0)$	Floquet state		
3	0.93126414831	0.71591	2.75993094140	0.71493	0.92721299001	0.70596	2.76506019467	0.71587
4	0.93126421515	0.71592	2.75993100922	0.71494	0.92721980937	0.70553	2.76506610221	0.71551
5	0.93126421517	0.71592	2.75993100923	0.71494	0.92721983293	0.70553	2.76506611450	0.71550
6	0.93126421517	0.71592	2.75993100923	0.71494	0.92721983278	0.70553	2.76506611427	0.71550
7	0.93126421517	0.71592	2.75993100923	0.71494	0.92721983293	0.71550	2.76506611450	0.70553

Number of rotor states	Two-photon resonance							
	$\omega = 0.0179332$ (a.u.)		$I = 0.1$ TW/cm ²		$\omega = 0.01793405$ (a.u.)			
	$\Phi(10^2)$	$\Phi(0)$	Floquet state	$\Phi(10^2)$	$\Phi(0)$	Floquet state		
3	0.93280668191	0.77773	4.51973680179	0.78137	0.93049663592	0.76661	4.52000298765	0.79582
4	0.93284750591	0.71769	4.51977095026	0.71950	0.93088762815	0.68103	4.52031701452	0.69558
5	0.93284753187	0.71776	4.51977097847	0.71956	0.93089014814	0.68172	4.52031963515	0.69624
6	0.93284753188	0.71776	4.51977097848	0.71956	0.93089015176	0.68172	4.52031963874	0.69624
7	0.93284753118	0.71776	4.51977097848	0.71956	0.93089015180	0.68172	4.52031963879	0.69624

(0,0) and at some later time t of still being found in this state: $|U_{00,00}(t)|^2$. The survival for state (0,0) is simply periodic and shows complete flow of probability out of and back into this state. However, the plot of $|U_{11,00}(t)|^2 = |U_{00,11}|^2$ shows that even though the flow of probability in (0,0) has a simple oscillatory form, the disposal of probability near the one-photon resonance is not excluded to state (1,1) because $|U_{11,00}(t)|^2$ never reaches more than 0.96. The survival of state (1,1) (Fig. 6), along with Fig. 5, shows best the multistate effects at high intensities. During what would otherwise be the Rabi cycles of the (1,1) survival probability there are times diminished probability. The transition probability, Fig. 4, indicates that while the majority of the probability flows to state (1,1) as much as 0.04 of the probability is disposed to other states.

D. Two-photon transitions

The $(2,2, \leftarrow 0,0)$ two-photon long-time-averaged transition probability versus field frequency is plotted in Fig. 7. The field-free resonance ω_0 is 0.035 866 4 a.u. ($\omega_0/2 = 0.017 933 18$). At 0.1 and 1.0 TW/cm^2 the resonance peaks are at 0.017 933 20 a.u. and 0.017 934 05 a.u., respectively. More will be said later about structure in this plot.

For the HF $(2,2 \leftarrow 0,0)$ two-photon transition at 1.0 TW/cm^2 , a plot of the transition probability (Fig. 8) reveals much more multistate interaction than for the one-photon resonance at the same intensity. This is to be expected in a two-photon reso-

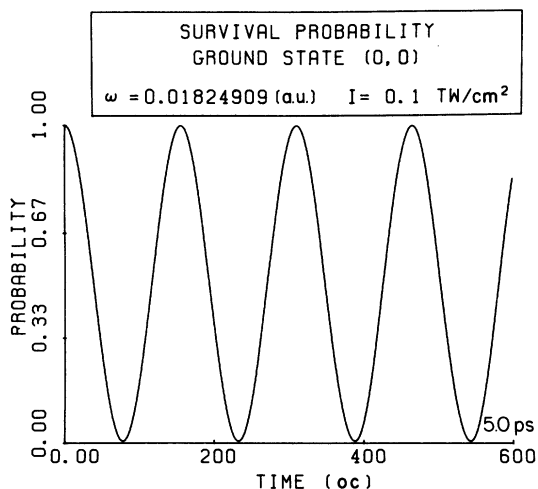


FIG. 5. Survival probability of the HF rotor ground state ($\nu=0, J=0$) for 600 oc (5.0 ps). Field frequency $\omega=0.018 249 09$. Intensity $I=1.0$ TW/cm^2 .

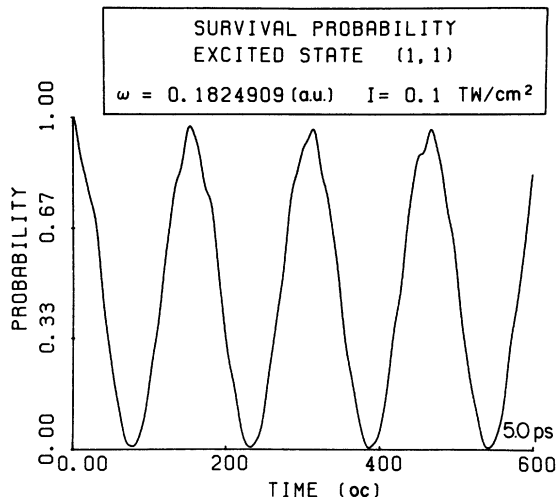


FIG. 6. Survival probability of the HF rotor state ($\nu=1, J=1$) for 600 oc (5.0 ps). Field frequency $\omega=0.018 249 09$. Intensity $I=1.0$ TW/cm^2 .

nance for which there is no matrix element directly connecting the initial and final state. Fig. 9 shows the long-time (up to 50 ps) dependence of this probability. This long-time structure has a period of 684 oc (5.79 ps) while the fine structure has a period of 49.7 oc (0.421 ps). Both the $(2,2)$ and $(0,0)$ survival probabilities also show this type of pattern.

Since we are particularly curious to know how accurately the interaction-picture second-order Magnus (IM2) expressions predict two-photon processes, the Magnus propagators were determined at times identical to those used by the numerical integration. To test the IM2 calculations against the

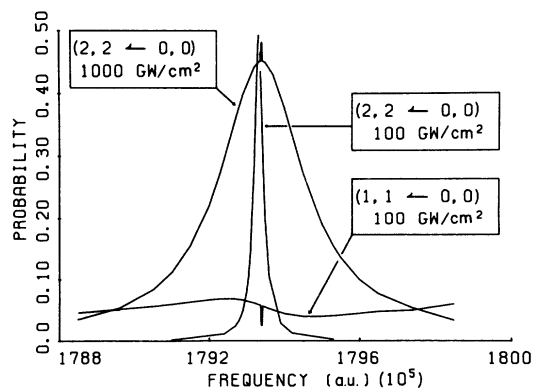


FIG. 7. The two peaks are two-photon absorption spectra for the resonant transition ($\nu=2, J=2 \leftarrow \nu=0, J=0$) at 0.1 and 1.0 TW/cm^2 . The shoulder of the $(1,1 \leftarrow 0,0)$ spectrum at 1.0 TW/cm^2 shows interaction between the one- and two-photon resonances.

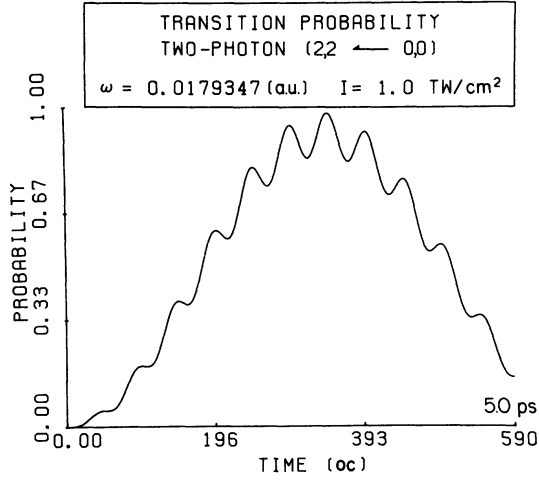


FIG. 8. Transition probability of the HF two-photon transition ($\nu=2$, $J=2 \leftarrow \nu=0$, $J=0$) for 590 oc (5.0 ps). Field frequency $\omega=0.0179347$. Intensity $I=1.0$ TW/cm².

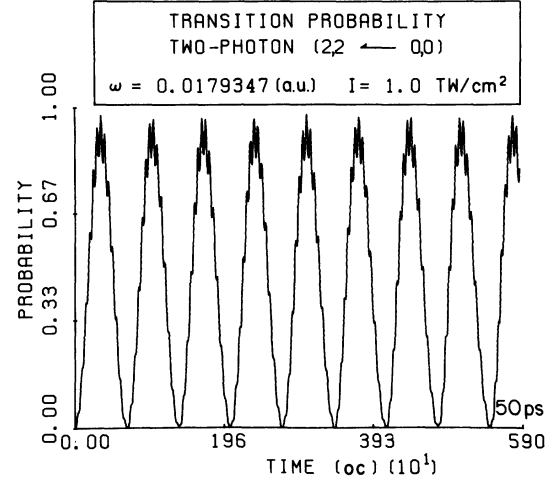


FIG. 9. Long-time transition probability of the HF two-photon transition ($\nu=2$, $J=2 \leftarrow \nu=0$, $J=0$) for 5900 oc (50.0 ps). Field frequency $\omega=0.0179347$. Intensity $I=1.0$ TW/cm².

NI results for the above one- and two-photon processes, the correlated Floquet energies and the mean energies [which will give an indication of $\Phi(t)$ accuracy] are listed in Table VI for both methods.

Table VI shows excellent agreement between the two methods for the characteristic values and the mean energies. The Floquet energies vary consistently by only five to six parts in 10^8 near the

TABLE VI. Floquet characteristic exponents (correlated) and mean energies for the two-photon transition ($\nu=2$, $J=2 \leftarrow \nu=0$, $J=0$): (IM2) determined by the second-order Magnus approximation of the interaction-picture propagator; (NI) determined by numerical integration in the interaction picture.

$\hbar\omega$ (a.u.)	$\gamma_{[0,0]} \times 10^2$ (a.u.)		$\gamma_{[2,2]} \times 10^2$ (a.u.)	
	NI	IM2	NI	IM2
0.017915	0.931 842 271 57	0.931 842 285 13	4.519 338 362 9	4.519 338 457 1
0.017920	0.931 717 079 73	0.931 717 097 99	4.519 472 754 4	4.519 472 843 8
0.017926	0.931 481 546 93	0.931 481 575 48	4.519 717 862 0	4.519 717 941 1
0.017932	0.931 080 340 57	0.931 080 386 81	4.520 127 071 6	4.520 127 133 0
0.0179331 76	0.930 974 865 09	0.930 974 915 49	4.520 233 933 6	4.520 233 990 8
0.0179337	0.930 924 727 64	0.930 924 779 92	4.520 284 669 7	4.520 284 725 0
0.0179339	0.930 905 076 74	0.930 905 129 74	4.520 304 545 9	4.520 304 600 5
0.0179340	0.930 895 144 57	0.930 895 197 93	4.520 314 590 2	4.520 314 644 4
0.0179450	0.929 422 409 30	0.929 422 493 35	4.521 797 052 4	4.521 797 075 9
0.0179500	0.928 584 870 63	0.928 584 961 13	4.522 637 322 4	4.522 637 339 4

	$\langle\langle H_{00} \rangle\rangle \times 10^2$ (a.u.)		$\langle\langle H_{22} \rangle\rangle \times 10^2$ (a.u.)	
	NI	IM2	NI	IM2
0.017915	1.304 234 326 8	1.304 221 753 5	4.111 972 677 9	4.111 986 439 1
0.017920	1.471 520 649 9	1.471 499 062 0	3.948 698 798 2	3.948 721 592 8
0.017926	1.837 543 626 0	1.837 502 680 8	3.587 409 572 5	3.587 451 744 7
0.017932	2.465 916 006 0	2.465 854 090 7	2.963 697 196 4	2.963 760 356 3
0.017933 176	2.613 535 976 0	2.613 472 432 4	2.816 983 259 5	2.817 048 050 8
0.017933 7	2.680 234 930 2	2.680 171 107 0	2.750 687 320 4	2.750 752 392 7
0.017933 9	2.705 750 408 2	2.705 686 553 6	2.725 325 555 3	2.725 390 659 6
0.017934 0	2.712 641 150 2	2.712 706 254 8	2.718 511 647 5	2.718 447 792 8
0.017945 0	3.809 163 675 4	3.809 134 487 2	1.630 365 478 4	1.630 395 941 1
0.017950 0	4.040 633 718 9	4.040 617 435 0	1.402 668 091 8	1.402 685 659 0

resonant frequency while away from resonance the variation is greater, and as large as nine parts in 10^8 . The mean energies agree for both methods, but the agreement is less than that of the FE's. This is probably due to the fact that in the Magnus A expressions many of the time-dependent expansion terms cancel at $t = \tau$: These time-dependent terms evidently converge slowly.

Also, the IM2 long-time—average probabilities agree with the NI results; they are not plotted because they are visually identical to the NI results of Figs. 3 and 7. A more detailed comparison of both the interaction and Schrödinger picture Magnus approximations with the NI results will follow in another paper.³¹

To accurately locate two-photon resonances in complex systems, computationally time-consuming spectra such as Figs. 3 and 7, are usually determined. However, the correlated Floquet characteristic exponents and the Magnus approximation provide an efficient method to locate resonances. A plot of the difference of the Floquet characteristic exponents for the two states involved in the transition $(2, 2 \leftarrow 0, 0)$ shows a parabolic minimum exactly at the position predicted by NI time-averaged calculations, $\omega_r = 0.0179332$ (see Fig. 10). For locating such resonances, then, the Magnus approximation would be more efficient than the NI method. It is only necessary to evaluate the propagator at $t = \tau$ (as opposed to integrating across the entire optical cycle), and to solve the eigenvalue equation (16). However, it is imperative to correctly make the correlation between the characteristic values and the

molecular energies, because there may be more than one pair of characteristic values that have a minimum very close to the resonance in question [e.g., for $(2, 2 \leftarrow 0, 0)$ there were four others].

Also, note that the minimum value is not zero; the Floquet characteristic exponents do not become identical at resonance. (In systems which do have degeneracy in the FCE's, i.e., identical FCE's, the application of Floquet theory will involve special theorems for degeneracy.¹⁰)

At 1.0 TW/cm^2 , the wing of the one-photon average transition probability versus field frequency (ω) slightly overlaps the two-photon spectrum (see Fig. 7). At the near-resonance frequencies for the two-photon transition, there is resonant interaction (RI) between the two- and one-photon process. The same effect occurs at 100 GW/cm^2 but it is almost an order of magnitude smaller. Because the HF spectra is free from any other comparatively intense absorption from the ground state and because the $(1, 1 \leftarrow 0, 0)$ structure is drastically changed only at frequencies near the $(2, 2 \leftarrow 0, 0)$ resonance, the interaction can be attributed to competition between the one and two-photon absorption.

In a previous paper⁷ the congested LiH spectra at 0.1 TW/cm^2 showed the same type of interaction, which we can now attribute to one, two, and three-photon processes involving resonance interactions. Also, in the multiphoton vibrational absorption spectra of OCS (Ref. 31) we have observed the same effect. Spectroscopically, for molecules with large dipole moment derivatives and at experimentally available intensities this structure could be detected. With HF, the detection of singly excited molecules, after pumping slightly below and above the two-photon resonance, should show, respectively, an enhanced or diminished intensity relative to the nonresonant shoulder intensity.

Figure 7 shows sharp spikes in the one- and two-photon absorption. Numerically, the two Floquet states involved in the resonance are not degenerate at these frequencies. The occurrence of these peaks over such a small frequency range is accompanied by a sharp change in the magnitude of the major Fourier components of $\Phi_{[11,00]}$ (from 0.2641 to 0.03644), $\Phi_{[22,00]}$ (from 0.6605 to 0.6948), and $\Phi_{[00,00]}$ (from 0.6885 to 0.7056). These components are over an order of magnitude larger than any others in the expansions. Also, the change in all other components is about two orders of magnitude less. It therefore appears at this point that the sharp peaks are also valid one- and two-photon resonance interactions, and are not indicative of numerical instability in the calculations.

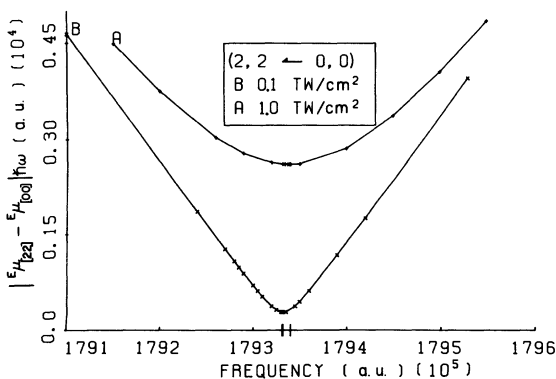


FIG. 10. Floquet characteristic exponent differences $|\mu_{[2,2]} - \mu_{[0,0]}| \hbar\omega$ near the two-photon $(2, 2 \leftarrow 0, 0)$ resonance at $I = 1.0 \text{ TW/cm}^2$. The Floquet characteristic exponents are those correlated to the molecular energies.

VII. CONCLUSIONS

The application of Floquet theory to the semiclassical interaction between a radiation field and a molecule provides a means to analyze the dynamics, as well as a method to derive all the dynamics through explicit consideration of interactions occurring within the first optical cycle (one field oscillation). The discovery of symmetry within the time dependence of the Floquet solution for Hamiltonians having the sinusoidal periodicity provides three new properties. These properties not only render computational checks but reduce the numerical effort of solving the equations of motion to only the *first half* of the optical cycle. Also, they simplify the complex eigenequation (used to obtain the Floquet characteristic exponents) into the diagonalization of a real matrix.

Using the Floquet characteristic exponents (FCE), the Floquet states may be labeled or mapped onto the molecular states by a process of zone extension of the Floquet energies ($\text{mod } \hbar\omega$) and correlation with the molecular energies. The molecular dynamics can then be sorted out in terms of the Floquet eigenvectors and eigenvalues, $[\Phi(0)$ and the FCE]. Single and multiphoton resonance can be located efficiently by the minimum of the FCE difference for two states associated with a resonance. Also, the mean energies of the Floquet states simply determine the stationary energy of the

fluctuating molecular-state energy. A study of these stationary energies should lead to accurate time-independent effective Hamiltonians.

Exact numerical calculations for intense IR irradiation of the HF vibrotor, using semiclassical radiation theory, are in good agreement with the second-order interaction-picture Magnus approximations for both one- and two-photon processes. The largest two-photon excitations from the ground state to the third vibrator manifold have dominated multistate contributions as shown by the dynamics. Within single-photon excitations, the multistate participation plays a relatively minor role in the dynamics. Resonance interaction between one- and two-photon excitations occurs at high intensities and causes noticeable asymmetry in the one-photon long-time—transition profile. This effect is observed in other molecules and should be physically measurable.

ACKNOWLEDGMENTS

We are indebted to Claude Leforestier for deriving Eq. (20) and supplying computer routines which saved us (and our Cyber computer) much time. This work was supported in part by research grants from the National Science Foundation and the Robert A. Welch Foundation.

-
- ¹M. G. Floquet, *Ann. Ec. Norm. Suppl.* **12**, 47 (1883).
²J. H. Poincaré, *Méthodes Nouvelles de la Mécanique Céleste*, Vol. I (Paris, 1892); *ibid.*, Vol. II (Paris, 1893); *ibid.*, Vol. III (Paris, 1899).
³W. R. Salzman, *Phys. Rev. A* **10**, 461 (1974).
⁴S. I. Chu and W. P. Reinhardt, *Phys. Rev. Lett.* **39**, 1195 (1977).
⁵S. I. Chu, *Chem. Phys. Lett.* **64**, 178 (1979).
⁶S. C. Leasure and R. E. Wyatt, *J. Chem. Phys.* **73**, 4439 (1980).
⁷S. C. Leasure, K. F. Milfeld, and R. E. Wyatt, *J. Chem. Phys.* **74**, 6197 (1981).
⁸C. Leforestier and R. E. Wyatt, *Phys. Rev. A* **25**, 1250 (1982).
⁹C. Leforestier and R. E. Wyatt, *J. Chem. Phys.* (in press).
¹⁰D. R. Dion and J. O. Hirschfelder, *Adv. Chem. Phys.* **35**, 265 (1976).
¹¹J. H. Shirley, *Phys. Rev. B* **138**, 979 (1965).
¹²V. I. Ritus, *Zh. Eksp. Teor. Fiz.* **24**, 1041 (1967) [*Sov. Phys.—JETP* **51**, 1544 (1966)].
¹³Ya B. Zeldovich, *Eksp. Teor. Fiz.* **24**, 1006 (1967) [*Sov. Phys.—JETP* **51**, 1492 (1966)].
¹⁴R. H. Young and W. J. Deal, Jr., *J. Math. Phys.* **11**, 3298 (1970).
¹⁵H. Sambe, *Phys. Rev. A* **7**, 2203 (1973).
¹⁶A. G. Fainshtein, N. L. Manakov, and L. P. Rapoport, *J. Phys. B* **11**, 2561 (1978).
¹⁷C. Cohen-Tannoudji, B. D. Lalöe, and F. Lalöe, *Quantum Mechanics* (Wiley, New York, 1977), translated by S. R. Homley, N. Ostrowsky, and D. Ostrowsky, pp. 381–314.
¹⁸F. R. Moulton, *Differential Equations* (MacMillan, New York, 1930), Chap. 17.
¹⁹S. Leasure and R. E. Wyatt, *Opt. Eng.* **19** **46**, (1980).
²⁰J. H. Shirley, Ph.D. thesis, California Institute of Technology, 1963 (unpublished).
²¹W. Magnus, *Comm. Pure Appl. Math.* **7**, 649 (1954).
²²C. Leforestier (private communication).

- ²³P. W. Langhoff, S. T. Epstein, and M. Karplus, *Rev. Mod. Phys.* **44**, 602 (1970).
- ²⁴F. J. Dyson, *Phys. Rev.* **75**, 486 (1949).
- ²⁵P. Pechukas and J. C. Light, *J. Chem. Phys.* **44**, 3897 (1965).
- ²⁶D. W. Robinson, *Helv. Phys. Acta* **36**, 140 (1963).
- ²⁷I. Scheck, J. Jortner, and M. L. Sage, *Chem. Phys.* **59**, 11 (1981).
- ²⁸P. S. Dardi and S. K. Gray have found differences between classical trajectory and quantum results for the HF vibrotor (unpublished results).
- ²⁹R. Bulirsch and J. Stoer, *Numer. Math.* **8**, 1 (1966).
- ³⁰M. Sargent III, M. O. Scully, and W. E. Lamb, Jr., *Laser Physics* (Addison-Wesley, Reading, Mass., 1977).
- ³¹K. F. Milfeld and R. E. Wyatt (unpublished).